Analysis of Unpowered Freewheeling Propeller Impact in Quadcopter for Energy Harvesting Process

Siranthini Balraj[#,*] and Anitha Ganesan[$]

[#]*Department of Electrical and Electronics Engineering, SRM Institute of Science and Technology, Chennai - 600 089, India*
[$]*Department Aerospace Engineering, Madras Institute of Technology, Anna University, Chennai - 600 044, India*
[*]*E-mail: sirajournal@gmail.com*

ABSTRACT

This research investigates the impact of freewheeling propellers in the Quadcopter for the purpose of harvesting energy. The main part of the Quadcopter is the propeller. In the arm of the Quadcopter, if the Unpowered freewheeling propeller is connected along with the main propeller at the time of Energy Harvesting (EH) process, the induced-flow caused by both propellers may interfere with the Quadcopter's aerodynamics. Consideration of the aerodynamic point of view to place the freewheeling propeller at a particular distance and place from the main propeller is very important. In this study, in terms of propeller diameter, two different types of freewheeling propeller designs are taken to investigation: Case 1- same size propellers and Case 2- different size propellers. Three distances between the main and freewheeling propellers are defined using the primary test setup as 8, 10, and 12 cm are taken to the software analyses using Computational Fluid Dynamics (CFD) ANSYS 18.1 / FLUENT simulation. The propeller airflow characteristics of pressure, force, and velocity variation between both cases are analysed using the graphical contour representation and measured values. The CFD simulation result showed that, Case 2-different size propellers got better force variation compared with the Case1-Same size propellers and 10 cm distance between the propellers in both the Cases seems good results compared with the other distances of 8 cm and 12 cm. This is an interesting design feature that can be used to locate the freewheeling propeller in the Quadcopter for Energy Harvesting purposes.

Keywords: UAV; Unpowered rotor; Freewheeling propeller; Quadcopter; CFD simulation; Energy harvesting

1. INTRODUCTION

Unmanned Aerial Vehicles (UAVs)[1] have inspired a lot of interest in recent years and have been deployed in a range of fields 1. A four-rotor aircraft, usually known as a Quadcopter or Quadrotor, is a Vertically Taking Off and Landing electric autonomous aircraft (VTOL). It's smaller and more structured than standard rotorcraft. The only disadvantage is the payload and power source limitations. Researchers have proposed a number of approaches for increasing the payload and power sources of Quadcopter using energy harvesting technology. Sowah Moses[2], *et al.* proposed that the Quadcopter's rotational energy could be used as an energy harvesting source, possibly increasing the flight time. A Brushless Direct Current (BLDC) generator plays a vital role to harvest the rotational energy into electrical energy. To optimise the harvested energy via BLDC generator many power maximisation techniques has proposed as the low-cost power maximisation conversion system by Halvaei Niasar [3], *et al.*, and sensorless PI and hysteresis comparator technique proposed by Damodharan[4], *et al.*

The majority of UAV, EH applications are solar or vibration energy harvesting, however, the recent research by Robert Swah[5], *et al.* shows that electrical energy may be directly harvested from continuously revolving components using the BLDC generator. In that paper it was achieved by 30 per cent of more current using the direct harvesting system setup resulting 10 min. implementation in Flight duration and were validated in the laboratory test setups. The BLDC generator power is not maximised in this design and more complex was mentioned to fix the generator directly to the rotational parts. Another way of utilising the rotational energy of the Quadcopter using the freewheeling Unpowered rotors.

The freewheeling Unpowered rotors are used in Rollefstad[6], *et al.*'s innovative design structure to boost the lift energy of the Quadcopter. By employing such structure, the wing plan form area has expanded, the lift energy has significantly increased, and as a result, less power is being used from the main battery. The same freewheeling energy harvesting technique proposed by Siranthini[7], *et al.* has been analysing the three various configurations and layouts to mount the freewheeling propeller in a proper place for energy harvesting process without affecting its actual design structure through the micro-BLOC generator. Out of three layouts, it was concluded and selected the layout-3 (up and down structure) for the rotational EH process. As per aerodynamic point of view, the thrust variation by the freewheeling propeller should not affect the main propeller thrust. The thrust variation had been analysed using the selected layout and resulted, layout-3 was given very minimum thrust

compared with other layouts. In this layout-3, the distance between the propellers cannot be adjustable but possible to keep a optimum fixed distance between the propellers. The main motivation of this investigation started from this point and derived the primary objective of this paper was to investigate the airflow characteristics between the main and freewheeling propeller in both cases and to select the optimum distance between them using CFD. Patel Karana[8], *et al.* employed CFD, a potent technique, as a prediction instrument in aerodynamics applications. Thanan Yomchinda[9], *et al.* analysed the design of UAVs, the airflow surrounding the airframe, propellers, and aerodynamic data using Computational Fluid Dynamics (CFD) techniques.

This paper is organised as follows: Section 2 presents the basic configurations of the proposed system and selection of the layout to the proposed plan; Section 3 provides the Propellers CAD model design and its implementation in ANSYS -Fluent Software. Section 4 briefs the simulation results and its description, the last section gives the result discussion and conclusion.

2. BASIC CONFIGURATIONS OF PROPOSED SYSTEM DESIGN

The BLDC generator is essential for energy harvesting purposes, and the rotating EH system that is directly coupled to the main motor shaft is being investigated[2]. The controlled rectifier[10] with sensorless technique[13] increases the power delivery from the BLDC generator. The three distinct layouts[11,12] have been evaluated and tested[7] in this work in order to place the freewheeling propeller for the EH applications. A comparison of the results [7] is shown in Table 1. The layout 3 (up and down structure), which offered the least amount of thrust variation and was chosen as the best for the suggested harvesting system without making much changes to the actual Quadcopter design, was determined by the results of the thrust tests. The main disadvantages of the selected layout-3,

according to the table results, are that the distance between the main and freewheeling propeller is too large, but that gap can be kept as a fixed one or optimised. To overcome this problem, the layout distance should be optimised.

Figure 1 shows the BLDC motor height (outside), shaft length, Quadcopter arm width, generator height, and tip distance were used to calculate the distance between the main and freewheeling propellers. These variables allowed the user to select the optimum distance. Three distances between the propellers 8, 10, and 12 cm were chosen for additional investigation using CFD modelling to identify the optimum distance after the preliminary test was carried out in the laboratory.
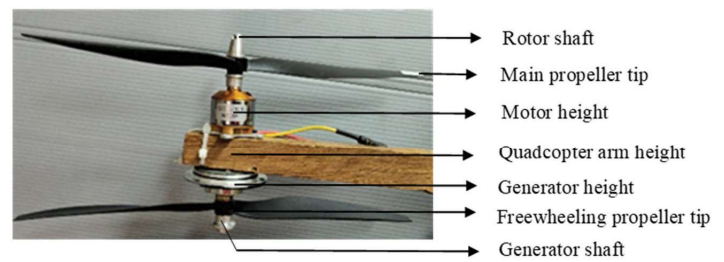

Figure 1. Gap distance deciding factors.

This study focused on two types of freewheeling propellers: same size Propellers, where the diameter of freewheeling propeller was identical to the main propeller. The main propeller dimension was 10X4.5 inch , i.e 10 inch diameter, 4.5 inch pitch variation. The another type named as different size propellers . In this type , freewheeling propeller diameter was less than the main propeller i.e 8X4.5 inch dimension. So there was 2inch variation between the propellers. The dimension of the propellers was chosen from the previous research work[6]. The airflow characteristics of pressure, velocity, and force distribution around both types of freewheeling propellers were analysed using the CFD simulation to get the optimum distance.

Table 1. Different layout comparisons

|	Layout 1	Layout 2	Layout 3
Connection	Motors along with free wheeling propellers in same single lengthy shaft (*Contrarotating*)	Motors and free wheeling propellersare mounted at the common supporting structure (*Upanddown*)	Motors and freewheeling propellers are mounted in a separate column facing each other (*Opposite*)
Advantage	• Clear inlet • Possible to adjust the distance • Does not change the original design of Quadcopter.	• Thrust and torque separated • Not having complex mechanics	• Thrust and torque separated • The distance between the propellers were freely adjustable
Disadvantage	• Lengthy inner shaft • Complex physical setup and mechanics • Very hard to separate the torque sand thrusts	• The distance between two propellers is too large • Distance cannot be adjustable • Possible to the optimum distance	• Strong • Rigid frame and supports need
Layout design			
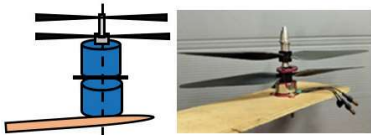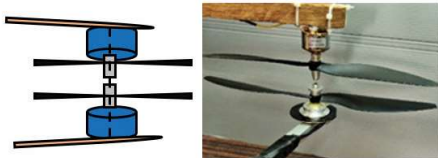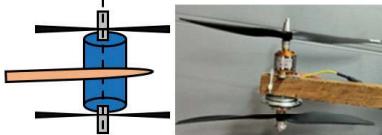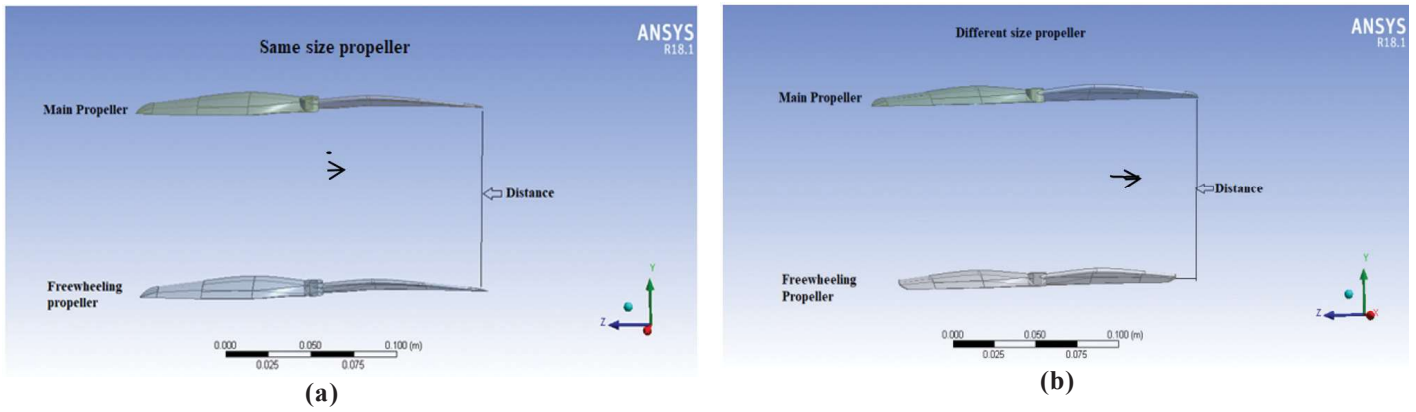
Figure 2. Propellers ANSYS workbench 18.1 model setup: (a) Same size propeller and (b) Different size propeller.
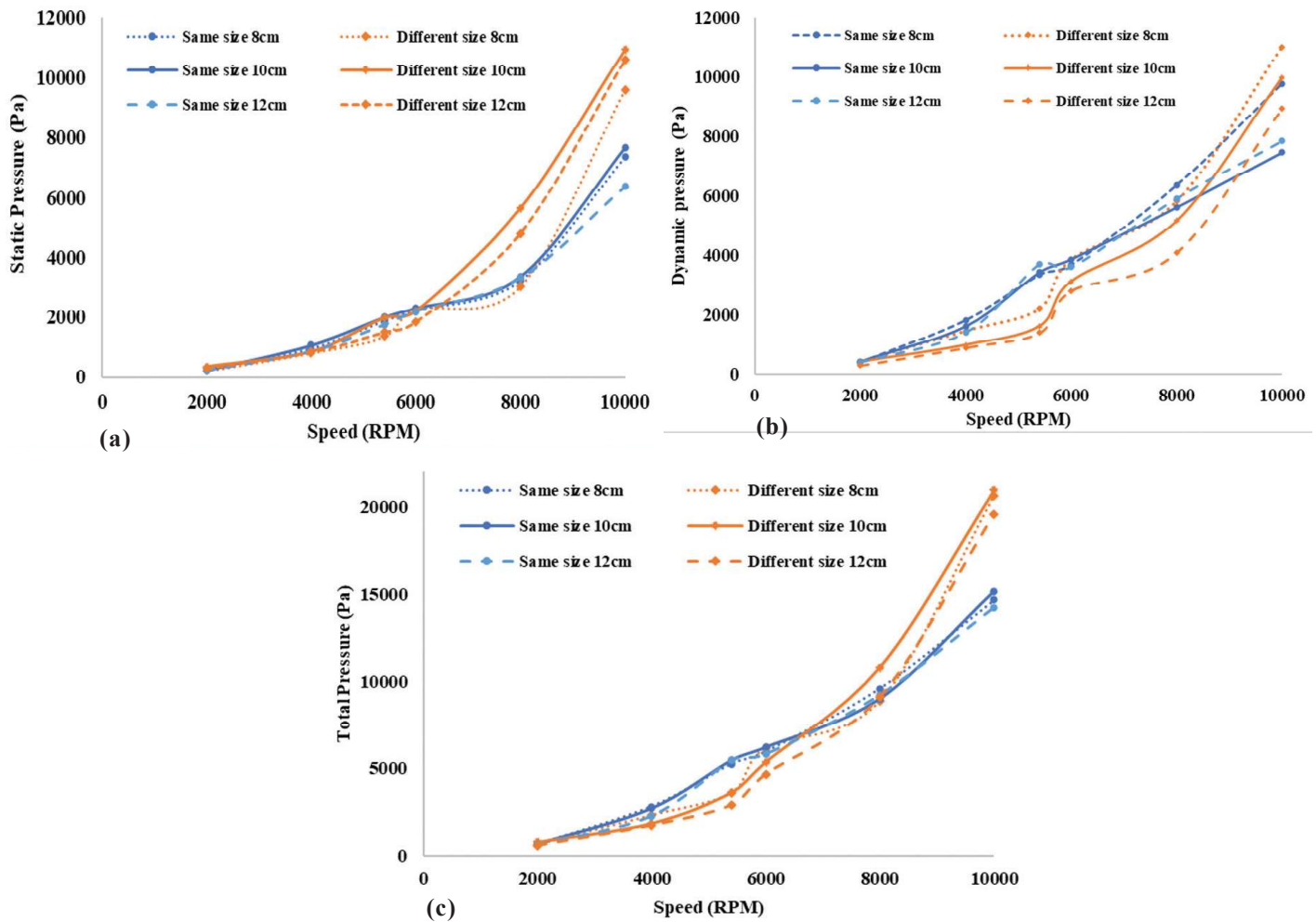

Figure 3. Propeller pressure variation with distances: (a) Static pressure (Pa), (b) Dynamic pressure (Pa), and (c) Total pressure (Pa).

3. PROPELLER CAD DESIGN AND CFD SIMULATION SETUP

The investigated propellers setup was drawn using CAD-CATIA software tool. Each airfoil data had been taken based upon the real propeller. The data[13] used to design the propellers are, Airfoil- NACA0021, Propeller - 10X4.5 inch, (Diameter:10-inch, pitch: 4.5-inch), Hub clearance - 3.7 mm, Nominal angular speed - 10000 RPM maximum, Propeller screw- 27 m/s. The selected airfoil designed by using CATIA for same and different size propellers, subsequently all the models with various distances of 8 cm, 10 cm, 12 cm was drawn, the geometry was updated into 'ANSYS FLUENT18.0' commercial CFD solver.

3.1 Propellers ANSYS Workbench Model Setup

ANSYS is the study simulation software for CFD, which gives better computational accuracy, fast modeling capabilities, and more optimised results[14]. Its workbench 18.1 version is used to set up the propeller's initial design, and the updated
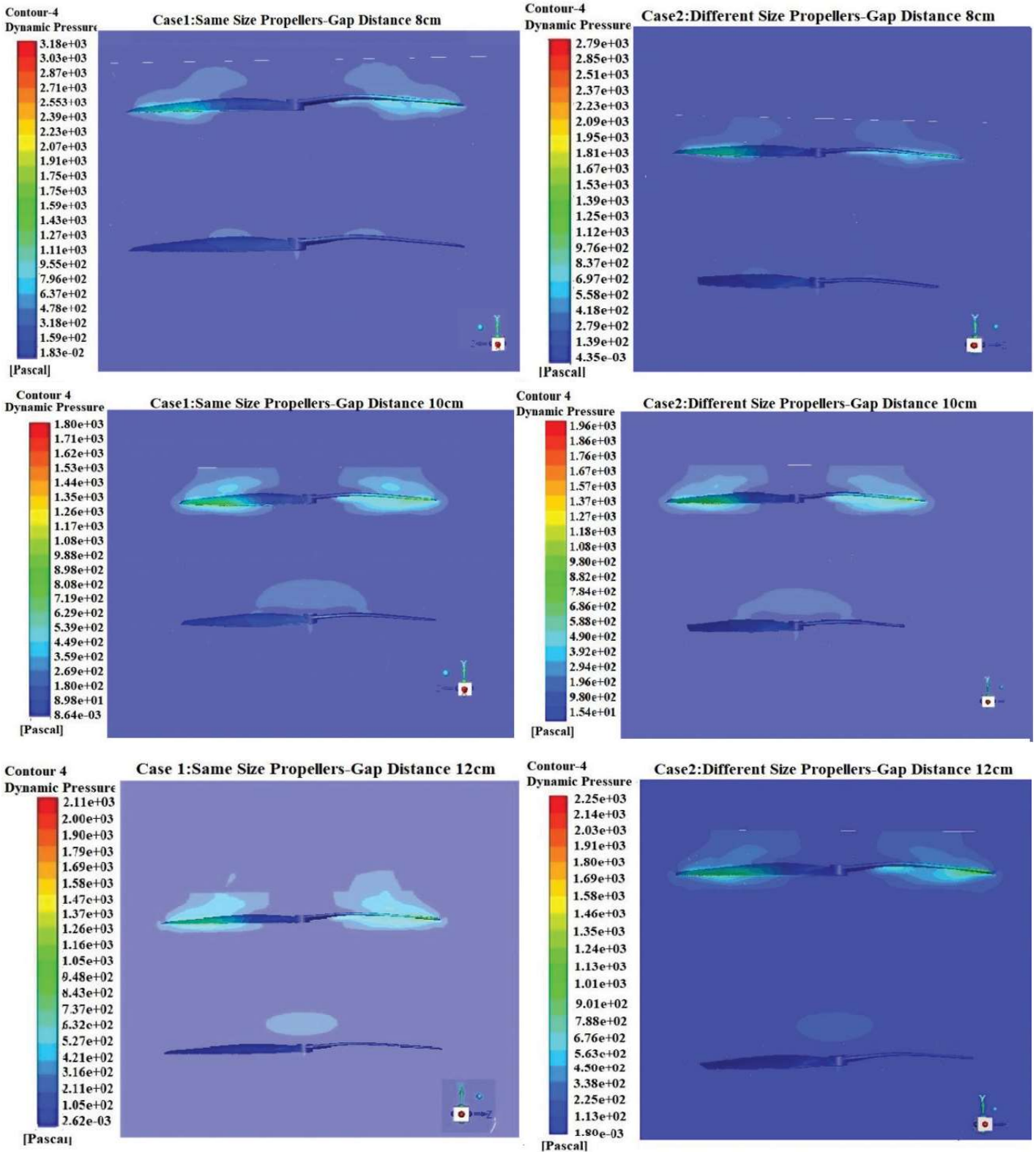
Figure 4. Dynamic pressure contour: Case 1 & Case 2.

propellers model is shown in Fig. 2(a) same size, Fig. 2(b) different size propellers.

The airflow around the propellers had been calculated numerically using the "Multiple Reference Frame model" (MRF) techniques. The grid was developed using a mesh tool in FLUENT 18.0. The matrix is dynamic since it produces each presentation of the geometry individually. The rate of convergences, the performance obtained from the numerical study, and the computational time required for the simulation were all directly impacted by the mesh structure. For the purposes of the current investigation, the size of the mesh cells was manufactured to a limited range along the main rotational propeller and to gradually increase towards the static domain of the freewheeling propeller.

By default, the FLUENT workbench might generate a conventional mesh with few elements. However, it's possible to manually restructuring the grid to generate mesh with a greater quality. Using minimum sizing, the number of cells can be raised even more by modifying the meshing parameter. The minimum sizing value was decreased to increase the number of cells, and vice versa. The best mesh size for the analyses is chosen based on computational timing to converge the solution and numerical accuracy.The static domain has 35 faces, 130 edges, and 80 vertices. The mesh was generated for further analysis and proceeded.

After meshing had done successfully, it moves to the setup for preprocessing control and define the initial parameters. For this analysis the type of solver took as "Pressure Based" . It was defined that the proposed design as a "Transient" time based and the Gravitational acceleration had given as "-9.81" in Y Axis, because the basic design of the model was in XZ plane. The input flow material defined as " air" and the other properties of density, specific heat, thermal conductivity and viscosity values are given as a standard which is inbuilt in the FLUENT solver. Two domains namely rotating domain (main propeller) and static domain (freewheeling propeller) are taken as for cell zone conditions. Here the mesh motion was initiated and the rotation axis direction gave in the Y axis. For any model the input and output conditions are determined using the "Boundary Conditions". To simplify the analysis the standard boundary conditions which is inbuilt FLUENT solver for the airflow analysis again was taken as input value.

3.2 CFD Simulation

The standard air density is 1.2 kg/m3, and the input air velocity was specified as 1 m/s. Minimal simulations were done at first to check the convergence of the residuals, and this procedure validated the meshes' proper operation. Results are more accurate when the convergence is higher and the residuals are decreasing more quickly. The input revolution speed was in the range of 2000 to 10000 RPM, and the solution was initiated for each rpm. When the input changed, the set of data was used to predict how the output would perform.To make the analysis simpler , two different types of Cases were used, namely:

- **Case1**: Same Size propellers with gap distance of 8 cm, 10 cm, 12 cm.
- **Case2**: Different Size propellers with gap distance of 8 cm,10 cm,12 cm.

The data was collected for three distances for both Cases after the Case had run each time with each RPM. The main propeller rotated when rotational speed provided to the rotating domain. The main propeller's air has created pressure, velocity, and force in response to the input speed. The following section describes in great detail on the corresponding simulation results.

4.   SIMULATION RESULTS
4.1 Pressure and Velocity Distribution

There are two types of pressure acting on the enclosure, i.e., the propeller's static and dynamic pressure.Static pressure is the local atmospheric pressure applied by the air to the walls perpendicular to the airstream. Dynamic pressure is the pressure associated with the flow motion caused by the air's kinetic energy that passes through the propeller. Dynamic pressure is directly related to the airspeed. The total pressure is the addition of static and dynamic pressure is given by the Eqn.,
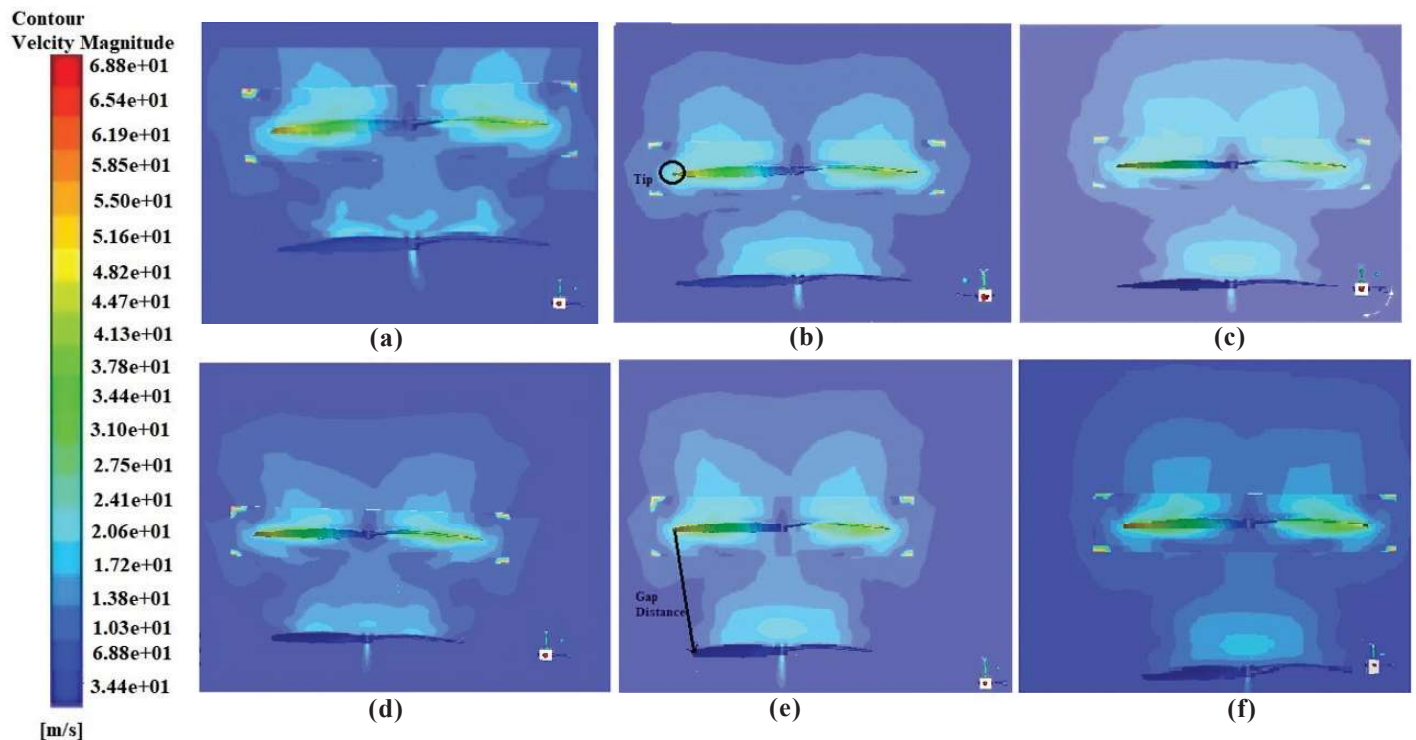
$$P_T = P_S + (0.5\ \rho\ V^2) \tag{1}$$

Figure 5. Velocity contour1-magnitude: Case1 (a), (b) & (c): Same size propellers - Gap distance (a) 8 cm (b) 10 cm (c) 12 cm; Case2 (d), (e) & (f): Different size propellers-gap distance (d) 8 cm (e) 10 cm (f) 12 cm.
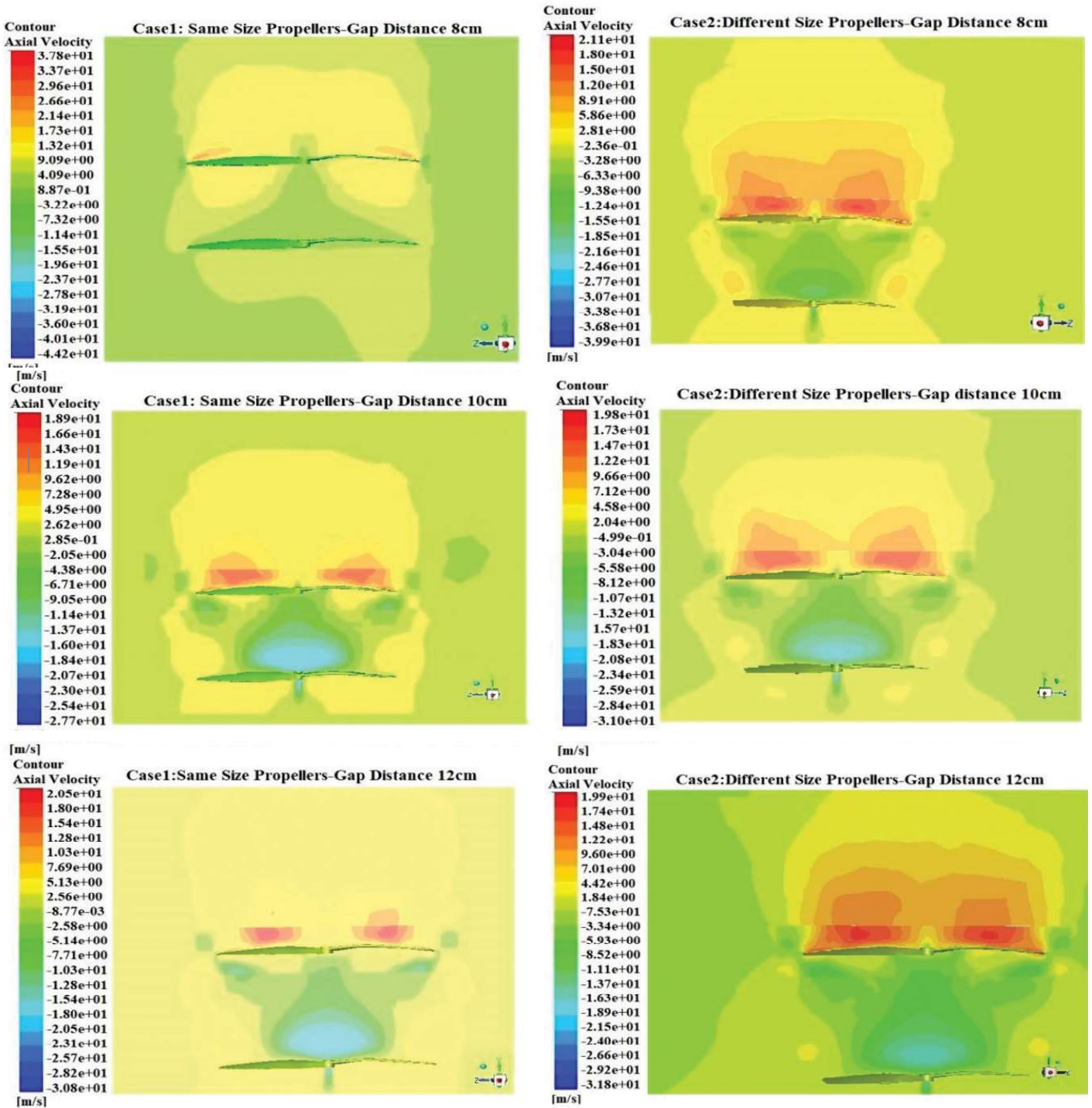
Figure 6. Velocity contour 2- Axial velocity: Case 1 & Case 2.

where,

P_T = Total pressure (Pa)
P_S = Static pressure (Pa)
ρ = Air density (kg/m³)
V = Input air velocity (m/s).

The velocity of airflow inside the enclosure was obtained by measuring the difference between the total (static and dynamic) and static pressure. When speed was given for each case one by one, the static, dynamic pressure, and velocity created by the main propeller at various distances for both the cases were shown in Fig. 3(a), Fig. 3(b) and Fig. 3(b).

The total pressure measurements in Fig. 3 (c) for speed variations indicated that Case-2 got more pressure than Case-1. The 10 cm gap distance reached relatively larger pressure at higher speeds when compared to other distances. Figure 4 depicts the dynamic flow characteristics for both Cases at the same speed (5400 RPM). The pressure difference was indicated by a colour variation. Different colours indicate the pressure fluctuations that occur around the moving propeller. On the left side of the scale, the maximum and minimum pressure variations that occurred during the simulation are displayed.

The pressure difference between the propeller's top and bottom surfaces generates the lifting force. According to the
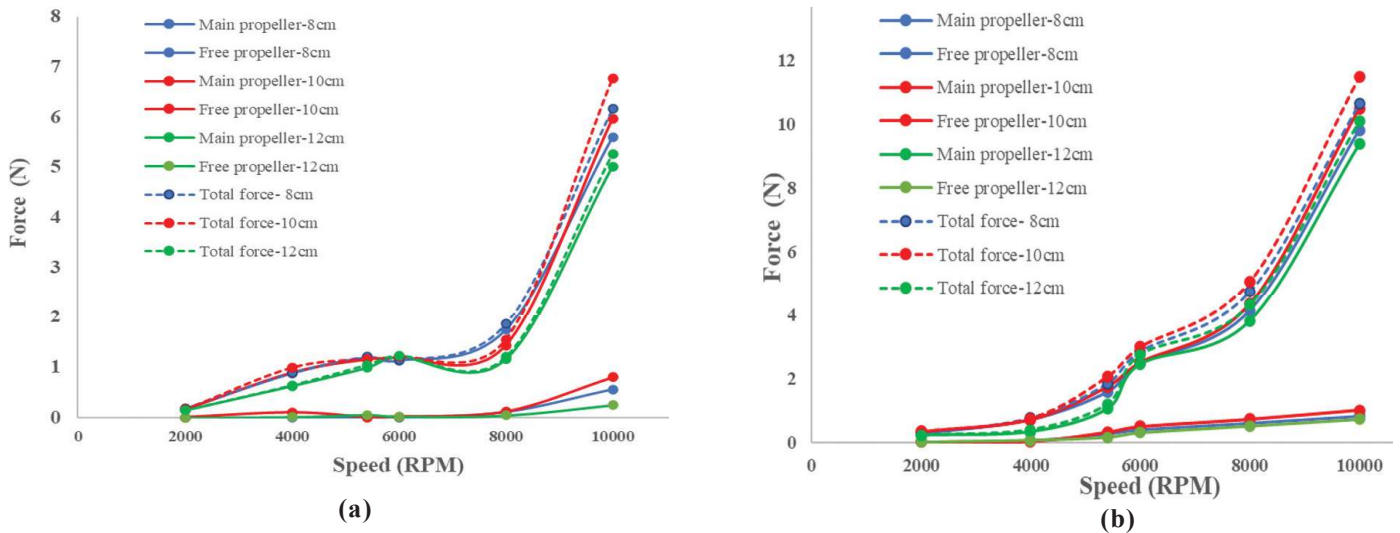
(a)

(b)

Figure 7. Force (N) variation with distances: (a) Case-1 (b) Case-2.

dynamic pressure contours in Fig. 4, the top surface of the propeller had lower air pressure than the bottom surface. The pressure difference produced the lift force of the propeller. The velocity contour shown in Figs. 5 and Fig. 6 as magnitude and axial velocity or Y-velocity, for the same speed (5400 RPM). In general, the air velocity flows more quickly on the top surface of the propeller. Higher-speed air molecules result in lower air pressure. For both cases, the distribution of the pressure difference that developed relative to the air velocity surrounding the propeller was determined.

The results of the velocity contours in Fig. 6 shown that different colour variations indicated different speeds around the propeller. The highest velocity is shown by the red colour variation, while the blue colour regions suggest a velocity effect in that section. The scale also showed the other colours and their equivalent velocity. Case-2 had a velocity distribution that is closer to the freewheeling propeller's edge (marked by a circle in Fig. 6 (b). In contrast, this was not in the Case-1 because primarily it is due to the diameter difference between the propellers. The air velocity at the propeller's tip possessed the maximum value. At simulation time, the tip velocity of the freewheeling propeller is observed using the velocity contour.

4.2 Force (n) Variation

A force produced by the main propeller on account of the air pressure reached the freewheeling propeller because of the high airflow pressure under the bottom surface of the main propeller. The main propeller's aid to the freewheeling propeller was seen in both cases at different speed . It's important to note that the main propeller force increased concurrently with the speed change. After the main propeller reached a specific speed 6, the freewheeling propeller started to turn. The freewheeling propeller was in a static state, but there was still a significant force drop to the surface of the blade. For Case-1 and Case-2, the data observation is represented by the graph in Fig. 7. The graph in Fig. 7 illustrates the data observation for Cases 1 and 2, respectively. The overall force was calculated as the sum of the forces exerted by the main and freewheeling propellers. The graph demonstrated how the force is increased in line with the input rotational speed. At lower speeds, the

force grew gradually; however, at higher speeds (about 8000 RPM), the force increased quickly, and with a gap distance of 10 cm, the combined forces of the main and freewheeling propellers were slightly higher in both cases. The combined force of the primary propeller and the freewheeling propeller was responsible for this.

4.3 Discussion of Results

Using CFD, the airflow characteristics of pressure, force, and velocity around the main propeller were examined for two Cases, with Case-2 outperforming Case-1 in terms of static and dynamic pressure created by the main propeller. The overall pressure variation for a 10 cm distance was slightly higher when compared to other distances. The velocity distributions for the two cases were identical as the gap distances changed. The overall force variation between the main and freewheeling propellers is moderate for a 10 cm gap distance at a higher speed. Moreover, Case-2's total force development had increased by an average of 56 per cent over case-1 as seen in Fig. 8.
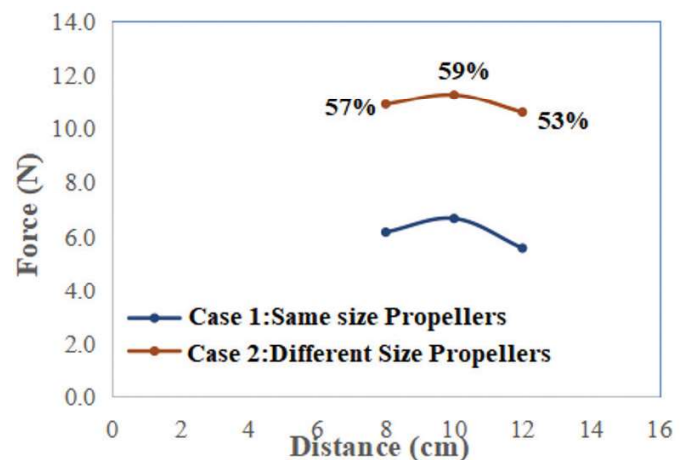

Figure 8. Force variation with distances.

This result demonstrated that a distance of 10 cm was optimal for obtaining a suitable resultant force for the freewheeling propeller, and the other distances of 8 cm to 12

9

cm were desirable for the freewheeling propeller to achieve better performance.

5. CONCLUSION

The distance between the propellers (main and freewheeling) is the most important factor in operating the Quadcopter's freewheeling rotational energy harvesting system without significantly altering its original design. The primary test configuration is used to determine three distances of 8, 10, and 12 cm, which are then examined using CFD–ANSYS 18.1 / FLUENT simulation. Case-1 for the same size and Case-2 for a different size with 8 cm, 10 cm, and 12 cm are the two test cases that were identified and examined. The airflow characteristics of pressure, force, and velocity change between the propellers were investigated using the graphical contour representation and observed values. In Case-2 compared to Case-1, the main propeller generated more static and dynamic pressure. The overall pressure variation over a distance of 10cm was slightly higher when compared to other distances. The overall force variation between the main and freewheeling propellers became moderate for a 10 cm gap distance at a higher speed. Moreover, Case-2 developed an average of 56 per cent more force overall than Case-1.Out of three distances that provided relatively high force at maximum speed, the optimum distance between the propellers was found to be 10 cm. Moreover, the freewheeling propeller offers good performance from an 8 cm minimum to a 12 cm maximum.Instead of diameter, variation in pitch and number of blades in freewheeling propeller needs to be analysed in future.

REFERENCES

1. Demir, K.; Cicibaş, H. & Arica, N. Unmanned aerial vehicle domain: Areas of research. *Def. Sci. J.,* 2015, **65**, 319-329.
   doi:10.14429/65.8631.
2. Sowah, R.; Acquah, M.A.; Ofoli, A.; Mills, G.A & Koumadi, M. Rotational energy harvesting to prolong flight duration of quadcopters. *IEEE Trans. Ind. Appl.*, 2017, **53**(5), 4965-4972.
   doi: 10.1109/TIA.2017.2698037.
3. Halvaei Niasar, A. & Sabbaghean, A. Design and implementation of a low-cost maximisation power conversion system for brushless DC generator, *Elsevier Ain Shams Eng. J.,* 2017, **8**(4), 571-80.
   doi: 10.1016/j.asej.2015.11.001.
4. Damodharan, P. & Vasudevan, K. Sensorless brushless dc motor drive based on the zero-crossing detection of back electromotive force (EMF) from the line voltage difference, *IEEE Trans. Energy Convers.* 2010, **25**(3), 661–668.
   doi:10.1109/TEC.2010.204178
5. Sowah, R.; Acquah, M.A.; Ofoli, A.; Mills, G.A & Koumadi, M. Rotational energy harvesting to prolong flight duration of quadcopters. IEEE Society Annual Meeting Conference , 2015, 1–7.
   doi: 978-1-4799-8374-0/15.
6. Rollefstad, S.B. Unmanned Aircraft System (UAS) with active energy harvesting and power management. US patent No: US 9,527,588 B1, December 27, 2017.
7. Siranthini, B. & Anitha, G. Indirect rotational energy harvesting system to enhance the power supply of the Quadcopter, *Def. Sci. J.*, 2020, **70**(2), 145-152.
   doi: 10.14429/dsj.70.14568.
8. Patel Karana, S. & Patel Saumil, B. CFD Analysis of an aerofoil, *Int. J. Eng. Res.*, 2014, **3**(3), 154-158.
   doi: 10.17577/IJERTCONV6IS14048
9. Thanan Yomchinda. Simplified propeller model for the study of UAV aerodynamics using CFD method, IEEE Conf., 2018, 69-74.
   doi: 10.1109/ACDT.2018.8592940.
10. Salinamakki, G.; Vivek, A. & Archana, S. Optimal energy harvesting from a high speed brushless DC generator-based flywheel energy storage system, *IET Electr. Power Appl.*, 2013, **7**(9), 693-700.
    doi: 978-1-4799-8586-9.
11. Storch, V.; Brada, M. & Nozicka, J. Experimental setup for measurement of contra rotating propellers, *Res. Gate Prague.*, 2017, 15-17.
    doi:10.14311/TPFM.2017.036.
12. Stephen. D. & Jonathon, C. Empirical measurements of small unmanned aerial vehicle co-axial rotor systems, *J. Sci. Innovation.*, 2011, **1**(1), 1-18.
    doi: 10.6654/JSI.201101_1(1).0001
13. Siranthini, B. & Anitha, G. Optimisation for augmentation of primary power supply to improve the endurance of the Quadcopter', industrial electrical power systems. *J. Electr. Eng.*, **19**(3), 2019 , 97-113.

CONTRIBUTORS

Dr Siranthini Balraj obtained his PhD in Avionics from Anna university and working as Assistant Professor in EEE, SRM Institute of Science and Technology, Ramapuram, Chennai. Her areas of interest are: Power optimisation, power applications of avionics, all electric aircraft.
In the current study she has contributed in the design and development of freewheeling energy harvesting system, laboratory tests, CFD simulation model design results.

Dr Anitha Ganesan obtained her PhD in Avionics from Anna University, Chennai and working as Associate Professor in Division of Avionics, Department of Aerospace Engineering, MIT, Anna University, Chennai. Her areas of interest are: avionics, aircraft navigation, guidance and control systems, and image processing.
In the current study she has contributed in the design and development of research overall methodology and guidance to improve the proposed method.